ELSEVIER

Chemical Engineering Journal 80 (2000) 3–12

Chemical Engineering Journal

www.elsevier.com/locate/cej

Bridging flocculation studied by light scattering and settling

Sharna M. Glover [a,*], Yao-de Yan [a], Graeme J. Jameson [a], Simon Biggs [b]

[a] *Centre for Multiphase Processes, Department of Chemical Engineering, The University of Newcastle, Callaghan, NSW 2308, Australia*
[b] *Centre for Multiphase Processes, Department of Chemistry, The University of Newcastle, Callaghan, NSW 2308, Australia*

Abstract

Polymers are used increasingly in solid–liquid separation processes. Bridging flocculation is the most common particle aggregation mechanism in these processes. However, little is known about the structure of the aggregates formed. This paper presents a critical comparison of two of the techniques that can be very useful tools for the characterisation of aggregate structures, i.e. static light scattering and settling. Of particular interest was their applicability for bridging flocculated aggregates. Both techniques were tested on two model systems: salt-induced fast coagulation and polymer-induced bridging flocculation of colloidal alumina particles. For diffusion-limited cluster–cluster aggregation at a high salt concentration, aggregate mass fractal dimensions of 1.75 and 1.65 were obtained from the light scattering and settling experiments, respectively. For bridging flocculation whereby flocs were formed using dual polymers, light scattering and settling gave mass fractal dimensions of 2.12 and 1.85, respectively. It was concluded that each of these techniques has certain advantages and disadvantages, therefore, it is best to view them as complementary. The settling method may be better suited for studying aggregates in bridging flocculation where floc sizes can be quite large which may cause the light scattering technique to become inapplicable.

Keywords: Bridging flocculation; Dual polymers; Mass fractal dimension; Static light scattering; Settling

1. Introduction

The process of bridging flocculation is applied in many industries to achieve efficient solid–liquid separations [1]. Applications exist in the mining, water and wastewater, pharmaceutical, and pulp and paper industries. The goal of bridging flocculation is the production of particle aggregates that have characteristics suitable for a specific application. Despite its wide application, bridging flocculation has not been understood as well as salt-induced coagulation. This is undoubtedly due to the fact that bridging flocculation is a highly complex process. Nevertheless, numerous studies have appeared in the literature [2–18]. These include studies of the flocculation kinetics [2,7,10,15], the conformation of the polymer at the surface [4,8,9], the electrostatic patch model [12,15–17], the mixing conditions [18], flocculation with very large polymers [3,6], the determination of aggregate density [14], and the aggregate structures using small-angle neutron scattering [11].

For many years, the structures of particle aggregates were non-classifiable in a mathematical sense. Yet, it is invaluable to gain this information in order to better understand and control the flocculation process. The advent of fractal mathematics to express the complexity of structures by Mandelbrot [19] has opened up a new and exciting pathway for the structural characterisation of particle aggregates. Fractal structures are self-similar, which means that their structure is invariant to a change of scale.

Light scattering has been used by an extensive number of researchers to probe the fractal properties of aggregates formed from a range of colloidal systems, using an array of system conditions. The majority of the studies have involved the aggregation of colloidal particles using a simple inert electrolyte. The two limiting regimes of diffusion-limited cluster–cluster aggregation (DLCA) and reaction-limited cluster–cluster aggregation (RLCA) have been well researched [20–27]. It is now generally recognised that DLCA and RLCA yield aggregate mass fractal dimensions of 1.75 and 2.1, respectively.

However, there exist certain criteria for the light scattering technique to be applicable to aggregate structure studies. That is, the aggregate has to obey the so-called Rayleigh-Gans-Debye criteria. In essence, there should be no multiple scattering or shadowing between the primary particles inside the aggregate. Several authors have investigated the effects that multiple scattering (light which is scattered more than once by the primary particles before reaching the detector) and shadowing (partial or total blocking of incident light) have on the applicability of light scattering for the

* Corresponding author. Tel.: +61-2-49216181; fax: +61-2-49601445.
E-mail address: swaters@mail.newcastle.edu.au (S.M. Glover).

1383-5866/00/$ – see front matter
PII: S1383-5866(00)00071-X

determination of aggregate structure [28–34]. The work of Lindsay and co-workers [28,31] suggests that multiple scattering has no effect on the measured scattering exponent in the fractal scattering regime. The consequences of shadowing are still unknown. Therefore, the use of light scattering for structural compactness determination is, in theory, only suited to small, open aggregates.

Settling is another technique that has been used in the literature for aggregate characterisation [14,35–49]. However, there has been considerable controversy for many years regarding the flow of fluid through aggregates and its implications on the analysis of settling data [36–38,42,43, 45,47–49]. Veerapaneni and Wiesner [38] have extensively modelled the permeability of an aggregate as a function of its radial distance using the Happel model and fractal geometry. Resistance to fluid flow through the aggregate was seen to increase with increasing fractal dimension, while for a given fractal dimension, the resistance to fluid flow was found to increase with increasing aggregate size. For aggregate to primary particle radius ratios of greater than 500 and fractal dimensions above 2, the aggregate was found to experience a force $\geq$95% of that experienced by an impermeable sphere of the same size. Therefore, for large and/or dense aggregates, there is expected to be very little flow through the aggregates.

In this study, a comparison will be made between the techniques of static light scattering and settling for aggregate structure characterisation. Aggregates were formed using DLCA and bridging flocculation experiments, and the respective aggregate mass fractal dimensions obtained from both techniques were compared. A discussion of the benefits and disadvantages of each technique is given. The applicability of each technique for the structure characterisation of bridging flocculated flocs was of particular interest. Some interesting observations on dual polymer induced bridging flocculation will also be discussed.

2. Background

2.1. Characterisation of aggregate structures using static light scattering

Particle aggregates formed from random aggregation processes are generally mass fractals. The mass, $m(R)$, of a mass fractal aggregate is proportional to its radius, R, to the power d_F:

$$m(R) \propto R^{d_F} \tag{1}$$

where d_F is the mass fractal dimension and corresponds to the degree of irregularity or the space-filling capacity of an object. The fractal dimension can be further related to the mass density of the aggregate, $\rho(R)$, as follows:

$$\rho(R) \propto R^{d_F-3} \tag{2}$$

Therefore, the mass fractal dimension gives a good indication of the structural compactness of the aggregate, with $1<d_F<3$ in three-dimensional Euclidean space.

Static light scattering experiments have been extensively used to probe the fractal nature of aggregates. The experiments are performed by directing a beam of light onto a sample and measuring the scattered intensity as a function of the magnitude of the scattering wave vector, Q. For a mass fractal aggregate which consists of monodisperse primary particles and which satisfies the Rayleigh-Gans-Debye (RGD) criteria, the scattered intensity $I(Q)$ from such an aggregate is given by [50]:

$$I(Q) = kP(Q)S(Q) \tag{3}$$

In the above equation, k is a scattering constant, $P(Q)$ is the single particle form factor and is related to the shape of the primary particle, and $S(Q)$ is the interparticle structure factor which describes the interference posed by the primary particles within the aggregate. Q is defined by:

$$Q = 4\pi n_0 \sin(\theta/2)/\lambda_0 \tag{4}$$

where n_0 is the refractive index of the dispersion medium, λ_0 is the wavelength of the incident light in vacuo, and θ is the scattering angle.

When $Qr_0 \ll 1$, where r_0 is the radius of the primary particles, the single particle form factor, $P(Q)$, becomes unity. Therefore, Eq. (3) can be written as:

$$I(Q) \propto S(Q) \tag{5}$$

In the region where $1/R \ll Q \ll 1/r_0$, the interparticle structure factor takes the form [50]:

$$S(Q) \propto Q^{-d_F} \tag{6}$$

Hence, Eq. (3) can be further simplified to give the following expression:

$$I(Q) \propto Q^{-d_F} \tag{7}$$

The fractal dimension can then be obtained from the slope of the $\log I(Q)$ versus $\log Q$ graph.

2.2. Characterisation of aggregate structures using settling

The number of primary particles, $N(R)$, within a mass fractal aggregate can be related to its mass fractal dimension, d_F, as follows:

$$N(R) \propto \left(\frac{R}{r_0}\right)^{d_F} \tag{8}$$

Assuming sphericity of the aggregate and no flow of solvent through it, in the creeping flow regime the following settling relationship can be established for the aggregate:

$$V_\infty \propto \frac{2}{9\mu_L} r_0^2 g(\rho_P - \rho_L) \left(\frac{R}{r_0}\right)^{d_F-1} \tag{9}$$

where V_∞ is the terminal settling velocity of the aggregate, μ_L is the viscosity of the solvent, ρ_L is the density of the solvent, ρ_P is the density of the primary particles, r_0 is the radius of the primary particles and g is acceleration due to gravity. By plotting the log of the terminal settling velocity versus the log of the aggregate size, the mass fractal dimension can be obtained.

Aggregates commonly have an ellipsoidal shape. It is therefore, necessary to convert the dimensions of the ellipsoidal aggregate into an 'equivalent sphere' diameter, that is, a sphere that would have the same settling velocity as that of the ellipse. The following equation, which is based on the work of Happel and Brenner [51], can be used to convert the dimensions of an ellipse to an equivalent sphere diameter:

$$d_{ST} = x\left(0.8248 + 0.168\left(\frac{y}{x}\right) + 1.033\times10^{-2}\left(\frac{y}{x}\right)^2 - 1.264\times10^{-3}\left(\frac{y}{x}\right)^3 + 3.728\times10^{-5}\left(\frac{y}{x}\right)^4\right) \quad (10)$$

where d_{ST} is the diameter of the equivalent sphere, and y and x are the maximum vertical and horizontal dimensions of the ellipse, respectively. Eq. (10) is valid for $0.1 \leq y{:}x \leq 20$.

In many industrial situations, the primary particles are polydispersed in size and therefore, the settling equation of the aggregate is best written in terms of an effective aggregate mass density, ρ_e:

$$V_\infty^2 = \frac{4 d_{ST} g}{3\rho_L C_d}(\rho_e - \rho_L) \quad (11)$$

where C_d is the drag coefficient for the equivalent sphere.

Using the above equation, the effective aggregate mass density can be calculated from the measured settling velocity of the aggregate and the diameter of the equivalent sphere. From the calculated effective mass density, the dry mass of the aggregate, $m(d_{ST})$, can be calculated using the following equation:

$$m(d_{ST}) = \frac{\pi d_{ST}^3 \rho_P (\rho_e - \rho_L)}{6(\rho_P - \rho_L)} \quad (12)$$

For objects settling within the creeping flow regime, that is, Reynolds number<0.1, the Stokes' law drag coefficient can be applied [51]:

$$C_d = 24\mathrm{Re}^{-1} \quad (13)$$

where

$$\mathrm{Re} = V_\infty d_{ST}\rho_L/\mu_L \quad (14)$$

For objects settling outside this regime, Jiang and Logan [52] have proposed the following drag coefficient for $0.1 < \mathrm{Re} < 10$:

$$C_d = 29.03\mathrm{Re}^{-0.871} \quad (15)$$

Therefore, calculation of the Reynolds number determines which regime the aggregates are settling in. Once the appropriate drag coefficient is calculated using Eq. (13) or Eq. (15), the effective aggregate density can be calculated from Eq. (11) and the aggregate dry mass calculated using Eq. (12). Based on Eq. (1), a plot of the dry mass against the equivalent sphere diameter on a double logarithmic scale will yield the aggregate mass fractal dimension.

3. Experimental

3.1. Materials

The high purity alumina (AKP-30) was supplied by Sumitomo Chemical Company and is reported to have a $d[50]$ value of approximately 0.4 μm. The alumina stock was prepared at a concentration of 5.0% w/w and was maintained at pH 5 to prevent aggregation. The particles were wetted for 4 weeks and sheared prior to use. Potassium nitrate (Ajax) was of an analytic grade and pH adjustment was conducted using potassium hydroxide (BDH) and nitric acid (BDH), both of analytical grade. The polymers trialed included a high molecular weight, 10% charge density anionic polyacrylamide (SNF Floerger), a very high molecular weight 100% charge density cationic polyacrylamide, and a polyacrylic acid of 30 000 molecular weight (Aldrich).

3.2. Alumina characterisation

The morphology of the particles was determined by scanning electron microscopy. The dried alumina powder was sprinkled onto a double sided sticky carbon tab which was attached to an aluminium pin stub. The sample was then sputter coated with about 20 nm of gold to prevent charging before viewing with a tungsten gun in a Philips XL30 SEM. Fig. 1 shows the photomicrograph of the alumina particles. The particles were also suspended at low pH and examined using the Mastersizer S light scattering device (Malvern Instruments, UK). The particle size distribution was found to be unimodal and the volume-derived diameter was 0.40 μm. The electrophoretic mobility values of the alumina particles as a function of pH were obtained using a Brookhaven Zetaplus instrument. A particle concentration of 5×10^{-3}% w/w and a fixed salt concentration of 10^{-4} M KNO_3 at 25°C were utilised in the mobility study.

3.3. DLCA and bridging flocculation experiments

DLCA was achieved by adding 50 ml of diluted alumina stock solution to 50 ml of 3 M KNO_3, both at pH 5, to give a particle concentration of 0.01% w/w. Trials were performed to achieve the most efficient bridging flocculation of the alumina particles at a solids concentration of 0.45% w/w. Cationic and high molecular weight anionic polymers were trialed separately and trials were also conducted using dual polymers. The most efficient flocculation was obtained with a dual polymer system. This involved

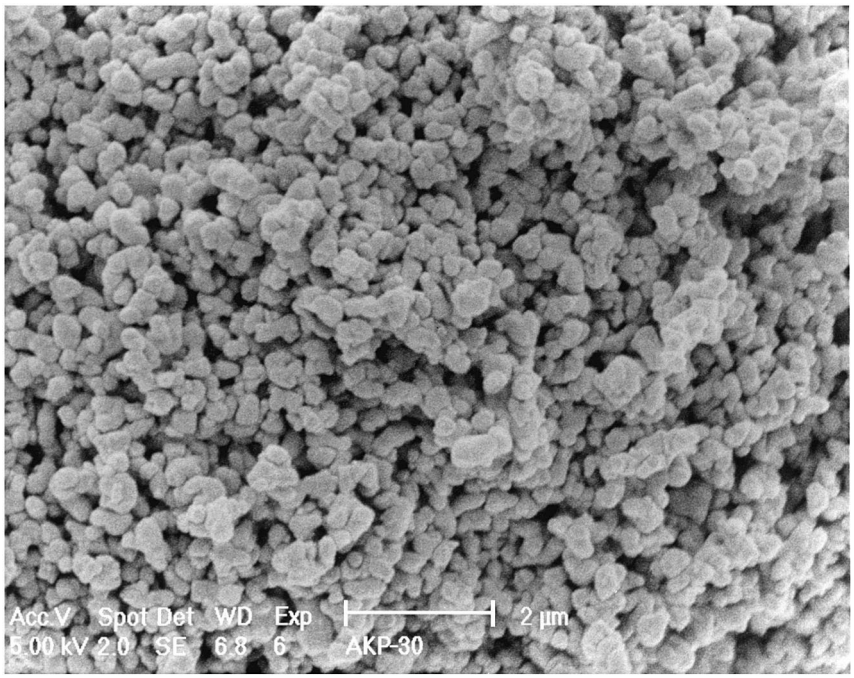

Fig. 1. Scanning electron micrograph of AKP-30 alumina.

dosing polyacrylic acid (PAA) first at a concentration of 0.2 ppm into the alumina suspension, which was maintained at pH 7.5. One minute was allowed to elapse before addition of the cationic polymer. The optimum dose of the cationic polymer was found to be 1.2 ppm.

3.4. Small-angle static light scattering

Small-angle static light scattering was employed to probe the fractal nature of the aggregates formed both from DLCA and bridging flocculation experiments. A Malvern Mastersizer S with a 633 nm He–Ne laser light source was used for the scattering studies. The instrument measures the scattered intensity at a range of scattering angles (0–46°). In addition, the Mastersizer is able to give approximate size information of the aggregates.

The DLCA experiment was performed by rapidly mixing the alumina and salt solutions and then gravity feeding a portion of the sample directly into the small volume cell of the Mastersizer. The coagulation kinetics were monitored over a period of 4 h under perikinetic conditions.

The bridging flocculation experiment was performed by adding the PAA to the alumina suspension, followed by the addition of the cationic polymer after 1 min under stirring conditions. The solution was then diluted by a factor of 100 and transferred into the magnetically stirred cell of the light scattering device. This cell allowed the sample to be slowly stirred and hence, the aggregates remained suspended while the size and intensity data were collected. Due to stirring, no change in aggregate size was observed over time.

3.5. Settling

Fig. 2 depicts the custom-built experimental settling apparatus. The column is surrounded by a water jacket and was maintained at 22°C. The column has internal dimensions of 20×20 mm. As such, the measured settling velocity will be in error by less than 5% due to wall effects for a 500-μm diameter aggregate. The aggregates can be viewed through a window at a distance of 200 mm from the entrance to the column. The aggregates were illuminated using a microscope light source (Zeiss). A trinocular head zoom lens (Edmund Scientific) mounted in the horizontal position was utilised to achieve the desired magnification. The lens gives 2.5 through to 10 times magnification at a constant working distance of 36 mm. The field of view available is 6.5–1.8 mm. The lens is mounted on two rack and pinion movements giving a possible 40 mm of travel in the horizontal direction and 105 mm in the vertical direction.

A monochrome CCD camera (Sony) was used to view the aggregates and their images were recorded on a VCR (Sony). The images were collected at 25 frames/s. A total magnification of 220–910 times was achieved on a large screen monitor (Sony). The equipment was calibrated using a 1-mm stage micrometer with 10-μm divisions. The aggregates obtained from both the DLCA and bridging flocculation experiments were gravity fed into the settling column which was pre-loaded with 1.5 M KNO_3 and distilled water, respectively. The aggregates were added to the column intermittently over a period of several hours and the run recorded on video tape. The vertical and horizontal dimensions as well as the settling velocities of the aggregates were

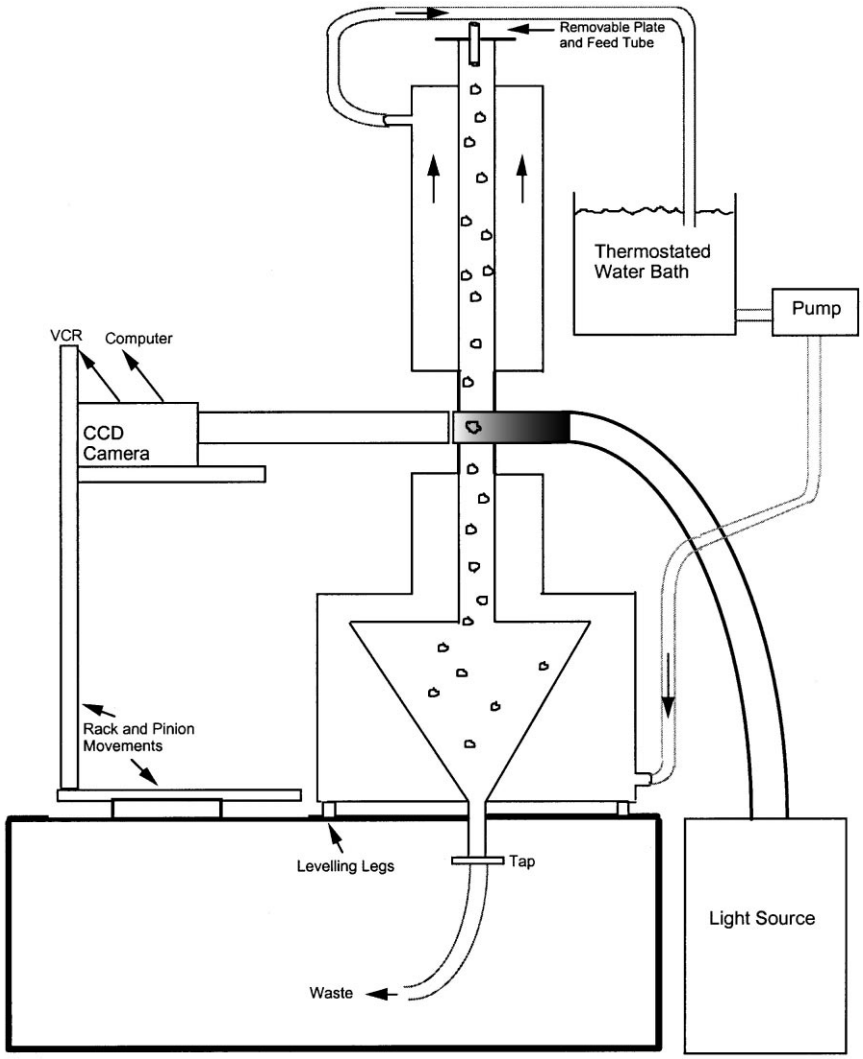

Fig. 2. Experimental settling device.

then measured. The computations involved the calculation of the equivalent sphere diameter, the effective aggregate mass density and the dry mass of the aggregate.

4. Results and discussion

The electrophoretic mobility of the alumina particles as a function of solution pH is shown in Fig. 3. The isoelectric point was found to occur at pH 9.5 with the surface maintaining a net positive charge below and a net negative charge above this pH value.

The growth behaviour of the aggregates with time when coagulating under the DLCA conditions is shown in Fig. 4. The light scattering intensity data produced from the DLCA aggregates with time are displayed in Fig. 5. A very linear region of the scattering curve was observed over one order of magnitude in Q. At the 1.5-h mark, the aggregates began to settle in the cell, as witnessed by the drop in the scattered light intensity.

The mass fractal dimension of the aggregates was obtained by applying Eq. (7) to the data in Fig. 5. The results are shown in Fig. 6 as a function of time. Before 40 min had elapsed, the aggregates had not grown to one order of

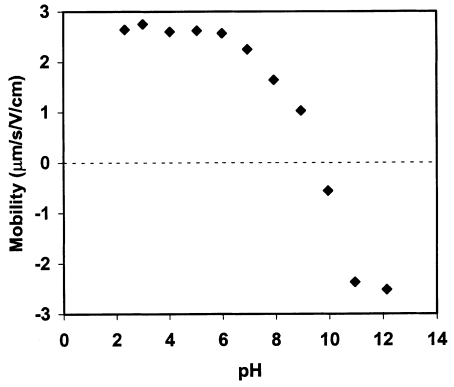

Fig. 3. The electrophoretic mobility of alumina particles dispersed in 10^{-4} M KNO_3 as a function of pH.

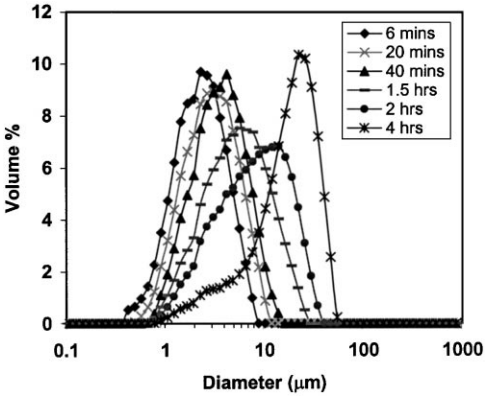

Fig. 4. Aggregate size distribution with time for the DLCA aggregates as obtained from light scattering.

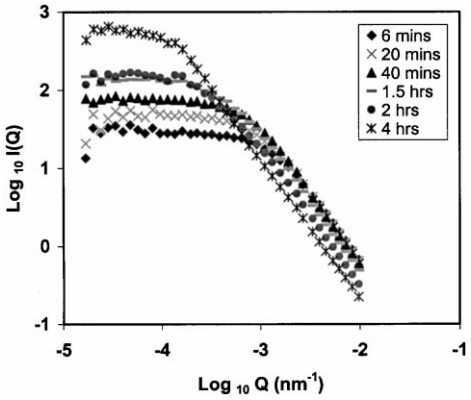

Fig. 5. Log $I(Q)$ versus log Q for the DLCA aggregates.

magnitude in size greater than the primary particles (cf. Fig. 4). Therefore, at these times it would be more appropriate to speak in terms of a scattering exponent rather than a fractal dimension. After 40 min, all aggregates were at least one order of magnitude in size larger than the primary particles and an average mass fractal dimension of 1.75 was obtained. The fractal dimension was seen to remain

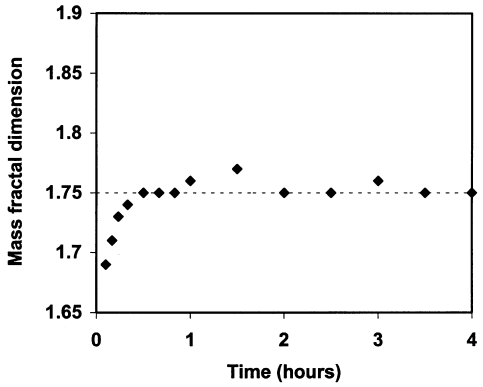

Fig. 6. Mass fractal dimension as a function of time for the DLCA aggregates as obtained from light scattering.

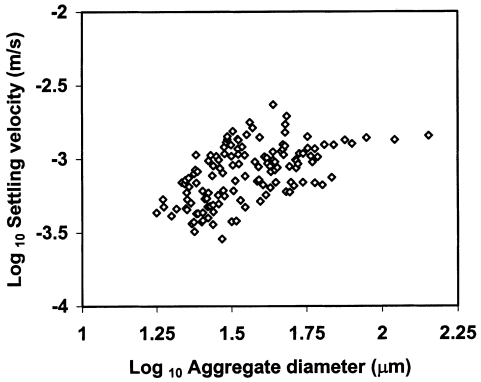

Fig. 7. Experimental settling velocity versus equivalent sphere diameter for the DLCA aggregates.

constant at approximately 1.75 with time, even after the 1.5-h mark when the aggregates were clearly settling. This result correlates well with the commonly recognised values of 1.75–1.80 for DLCA conditions [21,23].

Fig. 7 shows the experimental settling velocity values obtained for the DLCA aggregates. The effective aggregate density is plotted in Fig. 8 as a function of the equivalent sphere diameter. Fig. 9 shows the aggregate dry solid mass as a function of the aggregate diameter. Application of Eq. (1) gives a fractal dimension of 1.65. Several difficulties exist when using the settling technique to obtain fractal data from small, low density aggregates such as those generated from the DLCA conditions. Such aggregates are extremely sensitive to disturbances and therefore, there exists a degree of scatter in the data. The disturbances may originate exterior to the settling column, such as vibrations, or within the column itself due to possible movement of the supernatant.

Fluid flow through the DLCA aggregates could be expected to occur due to the low mass fractal dimension, that is, the high porosity of the aggregates. Based on the results of Veerapaneni and Wiesner [38], a simple analysis suggests that the DLCA aggregates would experience a force of between 0.875 (for small aggregates) and 0.925 (for

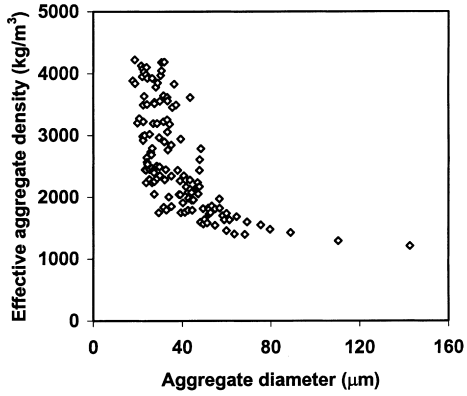

Fig. 8. Effective aggregate density versus equivalent sphere diameter for the DLCA aggregates.

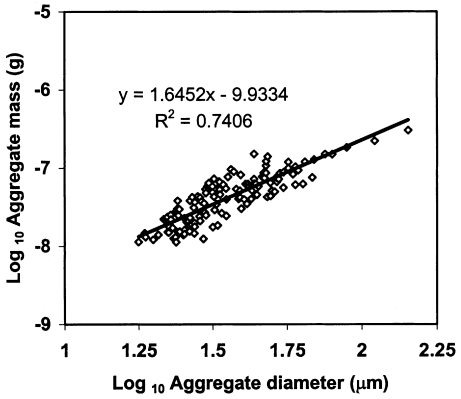

Fig. 9. Aggregate dry solid mass versus equivalent sphere diameter for the DLCA aggregates.

large aggregates) of that experienced by an impermeable sphere of the same size. Therefore, for the data shown here, the aggregate mass may well be overestimated. This will be more important for smaller aggregates. The net result is that fluid flow through aggregates may result in an underestimated mass fractal dimension. In the light of this, the fractal dimension obtained for the DLCA aggregates from the settling data is expected to be lower than that obtained from the light scattering method. A full analysis of each data point given here which allows for the flow through effect is beyond the scope of this paper. A full discussion of this point will be given elsewhere.

The settling experiments performed with the DLCA aggregates, for which the aggregate structure is well known from light scattering [21,23], proved that the technique used to obtain the mass fractal dimension of aggregates from settling data is valid. The settling technique was, therefore, extended to obtain aggregate structural information for bridging flocculated aggregates, and the results from both the light scattering and settling methods were also compared.

It proved difficult to achieve efficient bridging flocculation of alumina using a single polymer, as signified by fast settling aggregates and the acquirement of a clear supernatant. The results of flocculation with a range of polymers and polymer combinations are shown in Fig. 10. A brief discussion only of these results will be given below as the actual mechanisms of bridging flocculation are not the subject of this paper.

Addition of PAA was seen to cause some but inefficient flocculation. This is most probably due to an electrostatic interaction of the negatively charged polymer with the positively charged surface. The polymer will tend to adsorb at the particle surface in a flat conformation due to this attraction and hence, small patches of negative charge may reside on the particles. Flocculation can then result due to an electrostatic patch type model whereby the positive and negative patches of the particles come into contact, resulting in strong attachment [53].

Addition of the cationic polymer alone to the alumina at pH 7.5 resulted in some flocculation, which could be accounted for with a hydrogen bonding mechanism, since in this case, both surface and polymer were positively charged. The flocculation was poor, and the remaining supernatant was always turbid. The anionic polyacrylamide was also trialed at the same pH but also resulted in poor flocculation.

Dual polymer flocculation proved very successful when 0.2 ppm of PAA was followed by 1.2 ppm of the cationic polymer. The flocculation resulted in an improved supernatant clarity when compared to the use of a cationic or

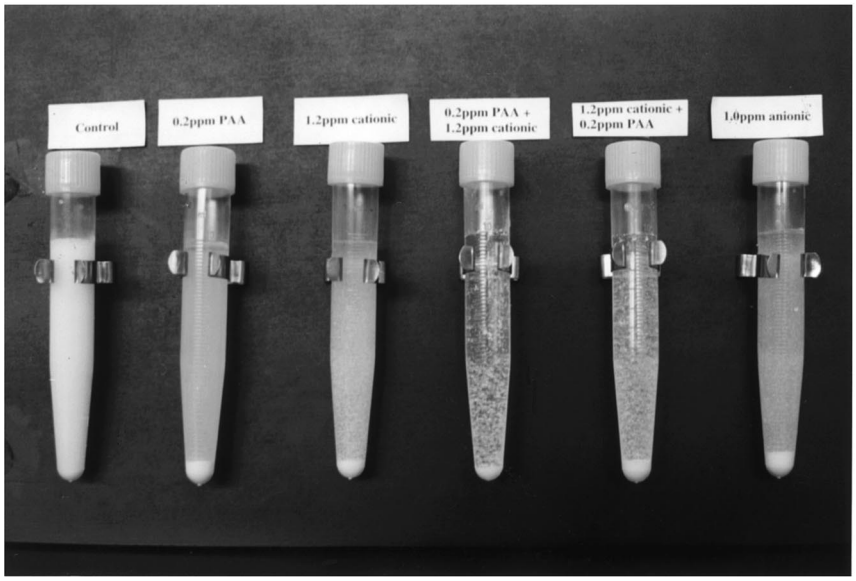

Fig. 10. Comparison of bridging flocculation regimes at pH 7.5. From left to right: control, 0.2 ppm PAA, 1.2 ppm cationic polymer, 0.2 ppm PAA followed by 1.2 ppm cationic polymer, 1.2 ppm cationic polymer followed by 0.2 ppm PAA, 1.0 ppm anionic polyacrylamide.

anionic polyacrylamide alone. Dual polymer flocculation whereby the cationic polymer was dosed prior to the PAA also resulted in improved flocculation in comparison to the use of the cationic polymer alone. However, as can be seen from Fig. 10, the flocculation was not as efficient when compared to the addition of PAA first. Interestingly, Yu and Somasundaran [54] obtained similar flocculation results when the order of polymer addition was reversed in their dual polymer studies. This can be explained by the higher solids concentration (2.6% w/w) employed in their experiments. It is likely that when the solids concentration is sufficiently high, the PAA when added second has a higher probability of encountering a particle first than encountering a cationic polymer molecule. In our experiments a solids concentration of 0.45% w/w was employed and therefore, some of the PAA polymer molecules may complex with the previously dosed cationic molecules prior to reaching any surface sites. This will tend to reduce the flocculation efficiency.

Due to the fact that the dual polymer system where the PAA was dosed prior to the cationic polymer consistently resulted in superior flocculation, these aggregates were chosen as the model for the bridging flocculation studies. Fig. 11 shows the aggregate size distribution, as measured from light scattering, resulting from this dual polymer experiment. The average floc size was 40 μm and the aggregate size distribution was unimodal. The scattered light intensity resulting from the aggregates is shown in Fig. 12. The slope shows a highly linear region over almost one order of magnitude in Q. However, the curve is seen to turn slightly upwards at large Q values. A clear explanation has yet to be found, but this could be due to correlations between the primary particles within the aggregate [11]. Light scattering yielded a scattering exponent of -2.12. Due to the limitations of the RGD theory when applied to large aggregates, one needs to be careful when equating the absolute value of this scattering exponent with the floc mass fractal dimension.

The experimental settling velocity values obtained for the bridging flocculated aggregates are presented in Fig. 13. The aggregate dry solid mass is given in Fig. 14(a) as a function of the equivalent sphere diameter, assuming creeping flow

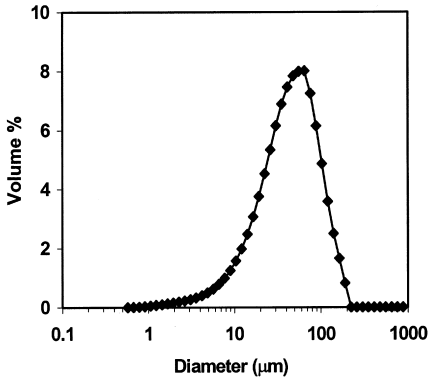

Fig. 11. Aggregate size distribution for the bridging flocculated aggregates as obtained from light scattering.

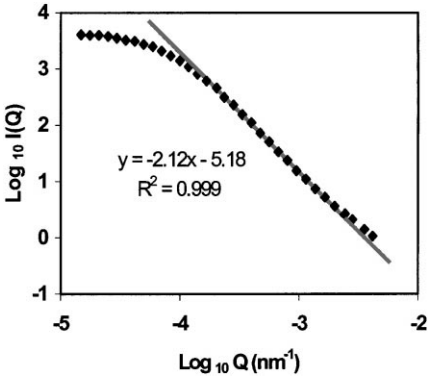

Fig. 12. Log $I(Q)$ versus log Q for the bridging flocculated aggregates.

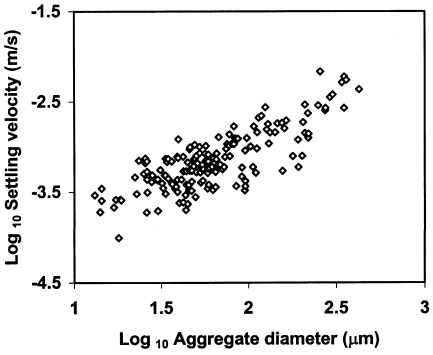

Fig. 13. Experimental settling velocity versus equivalent sphere diameter for the bridging flocculated aggregates.

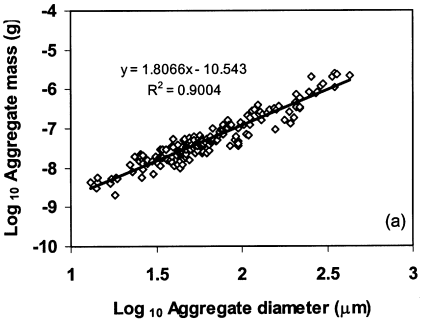

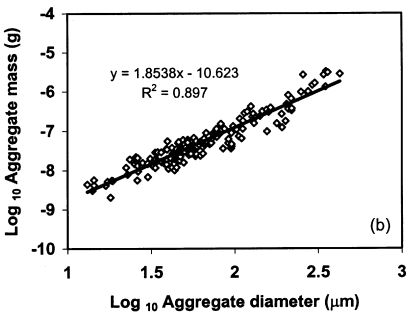

Fig. 14. Aggregate dry solid mass versus equivalent sphere diameter for the bridging flocculated aggregates: (a) $C_d=24\mathrm{Re}^{-1}$; and (b) $C_d=24\mathrm{Re}^{-1}$ for $\mathrm{Re}<0.1$ and $C_d=29.03\mathrm{Re}^{-0.871}$ for $\mathrm{Re}\geq 0.1$.

Table 1
Advantages of static light scattering and settling for the determination of aggregate structural compactness

Light scattering	Settling
Measurements are quick and data analysis straightforward	Aggregates are able to be directly visualised
Excellent technique for small, open aggregates	Excellent technique for large and/or dense aggregates (d_F>2)
The aggregation kinetics can be followed with time	Suitable for industrial samples which may contain dust particles
Analysis allows for the monitoring of aggregate restructuring with time	Suitable for aggregates formed from polydisperse primary particles

Table 2
Disadvantages of static light scattering and settling for the determination of aggregate structural compactness

Light scattering	Settling
Uncertainty in terms of possible shadowing effect for dense aggregates (d_F>2)	Measurements are time consuming
Not suitable for aggregates which settle quickly	Not suitable for very small or open aggregates as they are very susceptible to vibrations while settling
Difficult for industrial samples due to the presence of dust particles	Flow through the aggregate can cause errors to be introduced into small, tenuous aggregates
The effect of polydispersity of the primary particles on the measured fractal dimension is not well understood	Cannot be used for aggregates which restructure
Broad distribution in aggregate size or mass can introduce error into the measured slope	Not suitable for systems where the size distribution of aggregates is narrow

conditions for all sizes of aggregates. When compared to those obtained using the DLCA aggregates, it can be seen that the data contained much less scatter. This is partly due to the fact that the bridging flocculated aggregates were very large with a higher mass fractal dimension compared to the DLCA aggregates and therefore, the former were less susceptible to vibrations or fluid motion. The slope in Fig. 14(a) indicates a fractal dimension of 1.81. However, some of the bridging flocculated aggregates violated the creeping flow criteria. Fig. 14(b) presents the corrected data by using the drag coefficient given by Eq. (15) for aggregates with $Re \geq 0.1$, in conjunction with the creeping flow drag coefficient for aggregates with $Re < 0.1$. A fractal dimension of 1.85 was then obtained. Therefore, it is clear that an underestimated fractal dimension value results if creeping flow is wrongly assumed to apply to all aggregates.

Once again, as for the salt-induced aggregates, solvent flow through an aggregate may lead to errors in the settling velocities. As before, the aggregates may experience a force of 0.925 (for small aggregates) through to 0.985 (for large aggregates) times that of an impermeable sphere of the same size [38]. Therefore, due to the large size of the aggregates, the correction required for our bridging flocculated aggregates will not be as great as that required for our DLCA aggregates. Therefore, there would be very little increase in the fractal dimension of the bridging induced aggregates due to flow through the aggregates.

Tables 1 and 2 provide summaries of the advantages and disadvantages, respectively, of both the light scattering and settling techniques when used to determine the structural compactness of aggregates. The results obtained in this study indicate that light scattering and settling are very useful techniques for investigating the structures of particle aggregates. The two techniques are concluded to be complementary, with each being valid for a certain range of aggregate sizes and fractal dimensions. The settling technique is particularly well suited for bridging flocculated aggregates, whose sizes can be very large. As a result of these large sizes, static light scattering may become inapplicable.

5. Conclusions

This work has shown that static light scattering and settling are excellent techniques for investigating the structural compactness of particle aggregates. The use of light scattering for the determination of the fractal dimension of diffusion-limited cluster–cluster aggregates resulted in a value of 1.75. This result correlated very well with the literature values of 1.75–1.80 obtained by other authors using light scattering. Settling data from the DLCA aggregates were used to calculate the aggregate dry solid mass which could then be correlated with the aggregate equivalent sphere diameter. A fractal dimension of 1.65 was obtained from this method. However, due to the flow through these tenuous aggregates, the fractal dimension obtained from the settling data for such small, open aggregates may, if uncorrected, be underestimated. In the light of this, the resulting value of 1.65 obtained from the settling data can be concluded to compare well to that obtained from light scattering.

The comparison between the two techniques was extended to the case of bridging flocculated aggregates. An apparent value of 2.12 was obtained for the fractal dimension from light scattering. However, the aggregates were large in size and may thus violate the Rayleigh-Gans-Debye criteria. The

experiment was repeated and the fractal dimension calculated from the settling technique. When all of the aggregates were wrongly assumed to settle in the creeping flow regime, a fractal dimension of 1.81 was obtained. Re-calculation of the data using suitable drag coefficients resulted in a fractal dimension of 1.85. Therefore, application of the correct drag coefficient was proven to be essential.

The use of light scattering for the determination of aggregate compactness was concluded to be most applicable to small, open aggregates formed using model particles. The technique is fast and features such as aggregation kinetics and aggregate restructuring with time can be monitored. The use of settling for ascertaining aggregate structural compactness was deduced to be most suitable for large and/or dense aggregates which could either be formed using model particles or industrial samples. The technique is time-consuming but the aggregates are able to be directly visualised. It is especially useful for bridging flocculation studies where very large aggregates are normally formed so that the light scattering technique can become invalid.

Acknowledgements

S. Glover would like to thank the Australian Research Council for the award of an APA. The authors acknowledge the support of the Centre for Multiphase Processes, a Special Research Centre of the Australian Research Council.

References

[1] B.M. Moudgil, S. Behl, in: K.A. Matis (Ed.), Flotation Science and Engineering, Marcel Dekker, New York, 1995.
[2] C.C. Wu, C. Huang, D.J. Lee, Colloids Surf. A 122 (1997) 89.
[3] J.-P. Hsu, D.-P. Lin, Colloid Polym. Sci. 274 (1996) 172.
[4] X. Yu, P. Somasundaran, J. Colloid Interface Sci. 177 (1996) 283.
[5] Y.K. Leong, P.J. Scales, T.W. Healy, D.V. Boger, Colloids Surf. A 95 (1995) 43.
[6] W. Nowicki, G. Nowicka, Colloid Polym. Sci. 273 (1995) 298.
[7] Y. Adachi, M.A. Cohen Stuart, R. Fokkink, J. Colloid Interface Sci. 167 (1994) 346.
[8] K.F. Tjipangandjara, P. Somasundaran, Colloids Surf. A 46 (1991) 245.
[9] J. Blaakmeer, M.R. Bohmer, M.A. Cohen Stuart, G.J. Fleer, Macromolecules 23 (1990) 2301.
[10] E.G.M. Pelssers, M.A. Cohen Stuart, G.J. Fleer, J. Chem. Soc. Faraday Trans. 86 (1990) 1355.
[11] K. Wong, B. Cabane, R. Duplessix, J. Colloid Interface Sci. 123 (1988) 466.
[12] T.K. Wang, R. Audebert, J. Colloid Interface Sci. 119 (1987) 459.
[13] H. Hogg, in: B.M. Moudgil, P. Somasundaran (Eds.), Flocculation, Sedimentation and Consolidation, Engineering Foundation Conference, The Cloister, Sea Island, GA, American Institute of Chemical Engineers, New York, 1986.
[14] R. Hogg, R.C. Klimpel, D.T. Ray, in: B.M. Moudgil, P. Somasundaran (Eds.), Flocculation, Sedimentation and Consolidation, Engineering Foundation Conference, The Cloister, Sea Island, GA, American Institute of Chemical Engineers, New York, 1986.
[15] F. Mabire, R. Audebert, C. Quivoron, J. Colloid Interface Sci. 97 (1984) 120.
[16] A. Bleier, E.D. Goddard, Colloids Surf. 1 (1980) 407.
[17] K.W. Britt, Pulp Paper Can. 80 (1979) 67.
[18] G.J. Fleer, J. Lyklema, J. Colloid Interface Sci. 46 (1974) 1.
[19] B.B. Mandelbrot, The Fractal Geometry of Nature, W.A. Freeman, San Francisco, CA, 1982.
[20] R. Amal, G. Bushell, J. Colloid Interface Sci. 2 (1997) 37.
[21] J.L. Burns, Y.-D. Yan, G.J. Jameson, S. Biggs, Langmuir 13 (1997) 6413.
[22] M.Y. Lin, H.M. Lindsay, D.A. Weitz, R.C. Ball, R. Klein, P. Meakin, Phys. Rev. A 41 (1990) 2005.
[23] M.Y. Lin, H.M. Lindsay, D.A. Weitz, R. Klein, R.C. Ball, P. Meakin, J. Phys. Condens. Matter 2 (1990) 3093.
[24] J.E. Martin, J.P. Wilcoxon, D. Schaefer, J. Odinek, Phys. Rev. A 41 (1990) 4379.
[25] R. Zerrouk, A. Foissy, M. Rene, Y. Chevallier, J. Morawski, J. Colloid Interface Sci. 139 (1990) 20.
[26] V.A. Hackley, M.A. Anderson, Langmuir 5 (1989) 191.
[27] D.A. Weitz, M. Oliveria, Phys. Rev. Lett. 52 (1984) 1433.
[28] Z. Chen, P. Sheng, D.A. Weitz, H.M. Lindsay, M.Y. Lin, Phys. Rev. B 37 (1998) 5232.
[29] T.L. Farias, U.O. Koylu, M.G. Carvalho, Appl. Opt. 35 (1996) 6560.
[30] T.L. Farias, M.G. Carvalho, U.O. Koylu, G.M. Faeth, J. Heat Transf. 117 (1995) 152.
[31] H.M. Lindsay, M.Y. Lin, D.A. Weitz, P. Sheng, Z. Chen, R. Klein, P. Meakin, Faraday Discuss. Chem. Soc. 83 (1987) 153.
[32] D.A. Weitz, M.Y. Lin, H.M. Lindsay, J.S. Huang, Phys. Rev. Lett. 58 (1987) 1052.
[33] J.P. Wilcoxon, J.E. Martin, D.W. Schaefer, Phys. Rev. Lett. 58 (1987) 1051.
[34] D.A. Weitz, J.S. Huang, M.Y. Lin, J. Sung, Phys. Rev. Lett. 54 (1985) 1416.
[35] J. Gregory, Water Sci. Tech. 36 (1997) 1.
[36] X. Li, B.E. Logan, Environ. Sci. Technol. 31 (1997) 1229.
[37] C.P. Johnson, X. Li, B.E. Logan, Environ. Sci. Technol. 30 (1996) 1911.
[38] S. Veerapaneni, M.R. Wiesner, J. Colloid Interface Sci. 177 (1996) 45.
[39] C. Allain, M. Cloitre, F. Parisse, J. Colloid Interface Sci. 178 (1995) 411.
[40] C. Allain, M. Cloitre, M. Wafra, Phys. Rev. Lett. 74 (1995) 1478.
[41] S. Chellam, M.R. Wiesner, Water Res. 27 (1993) 1493.
[42] D. Li, J. Ganczarczyk, Water Res. 22 (1988) 789.
[43] B.E. Logan, J.R. Hunt, Limnol. Oceanogr. 32 (1987) 1034.
[44] J.B. Farrow, L.J. Warren, in: B.M. Moudgil, P. Somasaundaran (Eds.), Flocculation, Sedimentation and Consolidation, Engineering Foundation Conference, The Cloister, Sea Island, GA, Institute of Chemical Engineers, New York, 1986.
[45] M. Kajihara, J. Oceanogr. Soc. Jpn. 27 (1971) 158.
[46] J.H. Masliyah, M. Polikar, Can. J. Chem. Eng. 58 (1980) 299.
[47] K. Matsumoto, A. Suganino, Chem. Eng. Sci. 32 (1977) 445.
[48] G. Neale, N. Epstein, Chem. Eng. Sci. 28 (1973) 1865.
[49] D.N. Sutherland, C.T. Tan, Chem. Eng. Sci. 25 (1970) 1948.
[50] J. Teixeira, J. Appl. Cryst. 21 (1988) 781.
[51] J. Happel, H. Brenner, Low Reynolds Number Hydrodynamics, 2nd edn, Noordhoff International Publishing, Leyden, 1973.
[52] Q. Jiang, B.E. Logan, Environ. Sci. Technol. 25 (1991) 2031.
[53] J. Gregory, in: T.F. Tadros (Ed.), Solid–Liquid Dispersions, Academic Press, New York, 1987.
[54] X. Yu, P. Somasundaran, Colloids Surf. A 81 (1993) 17.